Journal of Catalysis **207,** 23–30 (2002)
doi:10.1006/jcat.2001.3502, available online at http://www.idealibrary.com on IDEAL®

Electrocatalytic Activity of Crystalline and Amorphous Nickel Model Alloys

Konrad Jobst and Hans Warlimont[1]

Institute of Solid State and Materials Research Dresden, P.O. Box 27 00 16, 01171 Dresden, Germany

Received July 30, 2001; revised November 1, 2001; accepted December 18, 2001

The influence of the chemical composition and structure of nickel base alloys on their catalytic activity was examined using the electrochemical reduction of 1-nitropropane as a test reaction. The electrocatalytic activity of cathodes consisting of crystalline and amorphous Ni-alloys, respectively, with systematically varying composition was analyzed. Aluminum, iron, and palladium were added as alloying elements. The effects of the nonmetallic components of the amorphous alloys, i.e., boron and silicon, which are required as glass formers, were also assessed. The results are discussed in terms of the effects of alloy composition and structure of the cathode materials on electrocatalytic hydrogenation and the electron transfer/protonation process at the cathode as a test reaction.

Key Words: **electrocatalysis; catalytic activity; Raney nickel; amorphous alloys; cyclic voltammetry.**

INTRODUCTION

The activity and the selectivity of Raney nickel catalysts for various reactions have been investigated as a function of the residual aluminum content after leaching. Since the different compositions of the precursor alloys and leaching conditions applied to activate the catalyst affect not only its final composition but also other properties such as the specific surface area, porosity, and surface oxidation, a direct correlation of the chemical composition of the metallic catalyst with its catalytic properties is virtually impossible. In order to distinguish the factors of influence, the present work is based on nickel alloys of different well-defined specimens which were prepared from the beginning with compositions close to those of activated Raney catalysts without undergoing the activation treatment. Accordingly, these samples, which had no porous, nanocrystalline microstructure, were subjected to a separate analysis of the effects of alloy composition, surface morphology, and other factors of influence. Both the classical method to manufacture metal strip through casting, rolling, and heat treatment and the preparation by high speed strip casting, the so-called rapid solidification technology, were used. The second mode of preparation can serve to produce an amorphous structure in alloys of suitably selected chemical composition. In this case metalloid elements such as silicon and boron are added in a relatively high concentration in order to achieve glass formation. Their content was typically in the 20 to 25 at% range. It was surmized that the metalloid components could affect the specific catalytic activity. Therefore, some alloys with variations in B and Si content were also investigated. Effects of B and Si have been observed, e.g., during the water electrolysis at electrodes consisting of amorphous metal-metalloid alloys (1).

The catalytic properties of amorphous metals and alloys have been reviewed by Molnár *et al.* (2) and Baiker (3). Numerous publications are concerned specifically with problems of their use as electrodes for electrocatalytic reactions which were reviewed critically by Tsirlina *et al.* (4). However, only very limited information has been generated so far which covers the effects of the chemical composition of alloy electrodes systematically and compares the catalytic activity of crystalline and amorphous electrodes, e.g., during electrochemical reduction reactions. In general, amorphous alloys are less active in conventional catalytic reactions and become effective only after a suitable surface treatment leading to an activated state (4, 5).[2] On the other hand, an activation treatment may not be required for some electrochemical reactions (4).

Vracar *et al.* (7) describe by way of theoretical considerations regarding hydrogen evolution at Pd–Ni electrodes the influence of the electrode properties on the electron transfer and the chemisorption on the electrode surface without discussing the different features of amorphous and crystalline surfaces. A very concise analysis of electrocatalytic hydrogenation is given by Robin *et al.* (6) in terms of the hydrogenation of unsaturated polycyclic aromatic compounds. They discuss the role of the cathode surface and

[1] To whom correspondence should be addressed. E-mail: warlimont@ifw-dresden.de.

[2] This surface activation should be distinguished from the activation treatment of Raney catalysts by treatment of a precursor alloy in an alkaline hydroxide solution, which leads to the conversion of the precursor alloy into a nanocrystalline nickel-rich and highly porous state.

0021-9517/02 $35.00

other factors of influence during electrochemical catalytic reduction. In particular, they differentiate between electrocatalytic hydrogenation (ECH), i.e., via transient hydrogen chemisorption at the catalyst surface, and the reduction by electronation–protonation (EP), i.e., by direct electron transfer, as the dominating mechanism.

In investigating the catalytic properties of amorphous metals and alloys, different authors have emphasized that rapid solidification technology permits to produce alloys with phase compositions and microstructures not accessible by conventional crystallization. Accordingly, this leads to materials with specific structures as well as electronic properties which can be analyzed regarding individual contributions to catalytic properties for specific reactions. Initially it was claimed that the unstable state of amorphous metal surfaces would be catalytically more active than their crystalline counterparts in general. However, by a number of investigations it was established that the amorphous state does not show a favorable influence on the reduction potential or the reaction yield in every case. It is surmized that the lower activity of amorphous alloys compared to that of Raney catalysts may be due to the absence of porosity in the amorphous state. But this would mean that crystalline alloys of corresponding composition should have a similarly low activity.

Considerable experimental work has been devoted to the use of amorphous electrodes in water electrolysis by Kreysa *et al.* (8–10). They studied the influence of the composition of amorphous Fe–Co and Ni–Co base alloys on the effectiveness of hydrogen and oxygen formation in alkaline media. The activity of amorphous alloy electrodes is higher due to the lower overvoltage compared to crystalline Pt or Ni electrodes. The electrodes were characterized by polarization curves and by means of cyclic voltammetry. Other authors found only negligible differences of the hydrogen evolution on crystalline and amorphous electrodes of alloys such as Ni–Zr, Cu–Ti, and Fe–Zr (11). A clear effect of the alloy composition was found with amorphous Cu–Ti which is discussed in terms of the dissociation energies of metal hydrogen bonds. Tsirlina *et al.* (4) examined specific properties of amorphous alloys modified by ion implantation. They assume—but do not show direct structural proof—that during the implantation of different ions "insular crystalline surface structures" are generated along with a high degree of segregation on amorphous surfaces which would determine the catalytic activity.

The catalytic effectiveness of amorphous alloys in organic oxidation or hydrogenation reactions was examined, among others, regarding the Fischer–Tropsch process or the hydrogenation of unsaturated hydrocarbons. In these cases only a few amorphous alloys were exhibiting favorable properties (12). However, a number of amorphous alloys are suitable as precursors for the production of highly active catalysts, as summarized by Baiker (3) where the formation of oxides with particular structures and electronic properties determine the catalytic behavior.

EXPERIMENTAL

Four kinds of metallic cathode materials were produced. Polycrystalline Ni–(Al,Fe,Pd) alloys (K series) were prepared by conventional induction melting, casting into a copper mold, rolling into strip form 10 mm in width and 0.2 mm in thickness, and final annealing treatment for recrystallization. One single crystal with a {111} surface was prepared (sample E1). Structurally, all crystalline alloys were solid solutions of the alloying elements Al, Fe, Pd in face-centered cubic Ni. The polycrystalline microstructure exhibited isometric crystallites with an average grain size of about 50 μm for pure Ni and 5–20 μm for the Ni base alloys. A typical microstructure is shown in Fig. 1.

Amorphous Ni–(Al,Fe,Pd)–Si,B alloys (N and L series with variations of the metallic and metalloid components, respectively) were manufactured by rapid solidification using a cooling wheel onto which the alloy was cast through a slitted nozzle in strip form, 10 mm in width and about (30 ± 5) μm in thickness. The structure was analyzed by X-ray diffraction. The samples were either fully or dominantly amorphous with minor fractions of crystalline phases present (10 to 30%) as indicated in Table 1.

The manufacturing process leaves the amorphous specimens with two different surfaces as shown in Fig. 2. These apparently different surfaces were investigated separately at higher microscopic resolution. The "shiny" side is the

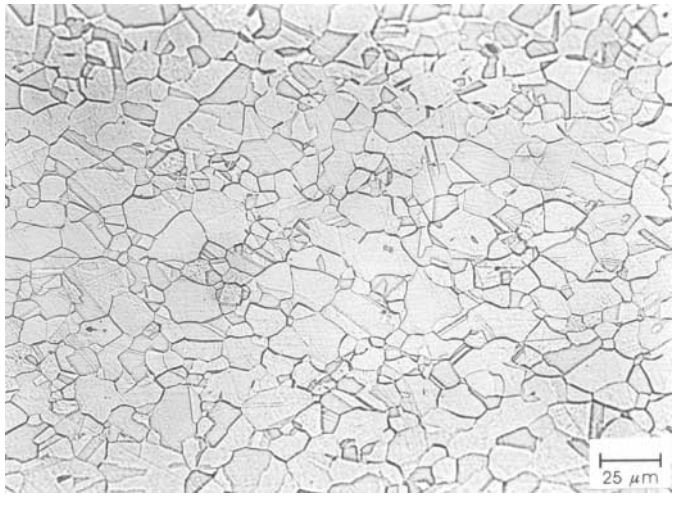

FIG. 1. Characteristic microstructure of a Ni–Al polycrystalline alloy cathode. Light micrograph.

TABLE 1

Chemical Composition and Structure of the Samples

No.	Sample designation	Composition [atomic%] Ni	Al	Fe	Pd	Si	B	Structure
K10	$Ni_{100.0}$	100	—	—	—	—	—	polycrystalline
K1	$Ni_{98.0}Al_{2.0}$	98.0	2.0	—	—	—	—	”
K2	$Ni_{95.1}Al_{4.9}$	95.1	4.9	—	—	—	—	”
K3	$Ni_{90.4}Al_{9.6}$	90.4	9.6	—	—	—	—	”
E1	$Ni_{94.1}Al_{4.5}Fe_{1.4}$	94.1	4.5	1.4	—	—	—	single crystal
K6	$Ni_{91.6}Al_{4.9}Fe_{3.5}$	91.6	4.9	3.5	—	—	—	polycrystalline
K7	$Ni_{99.5}Pd_{0.5}$	99.5	—	—	0.5	—	—	”
K8	$Ni_{99.0}Pd_{1.0}$	99.0	—	—	1.0	—	—	”
K9	$Ni_{98.1}Pd_{1.9}$	98.1	—	—	1.9	—	—	”
N10	$Ni_{74.4}Si_{7.7}B_{19.8}$	74.4	—	—	—	7.7	19.8	amorphous
N1	$Ni_{72.2}Al_{1.8}Si_{7.6}B_{17.9}$	72.7	1.8	—	—	7.6	17.9	”
N2	$Ni_{70.7}Al_{3.5}Si_{7.8}B_{18.0}$	70.7	3.5	—	—	7.8	18.0	”
N3	$Ni_{68.0}Al_{6.9}Si_{7.5}B_{17.6}$	68.0	6.9	—	—	7.5	17.6	”
N6	$Ni_{68.6}Al_{3.5}Fe_{2.7}Si_{7.7}B_{19.8}$	68.6	3.5	2.7	—	7.7	19.8	”
N7	$Ni_{74.6}Pd_{0.3}Si_{7.8}B_{20.0}$	74.6	—	—	0.3	7.8	20.0	”
N9	$Ni_{72.5}Pd_{1.4}Si_{7.8}B_{20.0}$	72.5	—	—	1.4	7.8	20.0	”
L18	$Ni_{72.6}Al_{3.8}B_{23.6}$	72.6	3.8	—	—	—	23.6	ca. 60–70% amorphous
L19	$Ni_{70.0}Al_{3.7}B_{27.3}$	70.0	3.7	—	—	—	27.3	ca. 80% amorphous
L20	$Ni_{68.8}Al_{4.0}Si_{19.5}$	68.8	4.0	—	—	19.5	—	n. a.
L21	$Ni_{72.5}Al_{3.9}Si_{24.2}$	72.5	3.9	—	—	24.2	—	ca. 10–20% amorphous

free surface in the casting process which has solidified in contact with air and is essentially smooth; the “dull” side is the surface which has solidified in contact with the cooling wheel; its roughness is caused partly by the surface of the cooling wheel and partly by the inclusion of air between the cooling wheel and the strip as it forms. On the scale of resolution of an atomic force microscope the specimens were essentially smooth. All samples were analyzed chemically by standard methods. The results are given in Table 1.

In this investigation, cyclic voltammetry (CV) was employed to test the catalytic activity but only the reduction branch was evaluated. The reverse scan is omitted in the representation of the results. The alloys listed in Table 1 were used as cathodes for the electrochemical reduction of 1-nitropropane as a test substrate in aqueous electrolytes at $p_H = 1.0$ and $p_H = 6.8$, respectively. The 1-nitropropane reduction reaction was applied as an indicator of the effects of different structural states—amorphous or crystalline—and alloy concentrations. The electrochemical reduction of nitrobenzene, which is generally used to characterize Raney nickel catalysts, e.g. (15), is poorly reproducible in CV measurements since the potential/current curves are partially irreversible. Therefore, this test reaction was not applied here. The complete possible reduction sequence of 1-nitropropane is illustrated in Fig. 3 according to a survey of the electrochemical reduction of aliphatic nitro compounds (14). The possible alternative reduction sequences of 1-nitropropane $C_3H_7NO_2$ may be described as follows:

EP-mechanism	ECH-mechanism
First reduction step	
$C_3H_7NO_2 + 2H^+ + 2e^- = C_3H_7NO + H_2O$	$2H^+ + 2e^- = 2H$ $C_3H_7NO_2 + 2H = C_3H_7NO + H_2O$
Second reduction step	
$C_3H_7NO + 2H^+ + 2e^- = C_3H_7NHOH$	$2\,H^+ + 2e^- = 2H$ $C_3H_7NO + 2H = C_3H_7NHOH$

The potential of the cathode was varied continuously at a constant rate starting from 0 V vs NHE to a potential of −1.25 V vs NHE while the current density was measured. Subsequently the potential was reset to 0 V and kept constant for a predetermined time for equilibration to be attained before a new cycle was started. In this case, at a finite scan rate, the curves $j = f(E)$ have the form shown schematically in Fig. 4. The peak cathodic potentials E_p^c at the minima of the current density, two reduction peaks occurring at $p_H = 1.0$ one at $p_H = 6.8$, respectively, were used as indicators of the activity of the cathode regardless of which of the individual peaks was attributed to a particular electrochemical reduction reaction of 1-nitropropane. Aqueous solutions of 1-nitropropane are saturated at 0.157 mol l^{-1} at room temperature. In order to increase the conductivity, 0.25 mol l^{-1} of potassium sulphate was added to the electrolyte.

The electrochemical investigations were carried out using a computer-controlled potentiostat PS6 (Meinsberg)

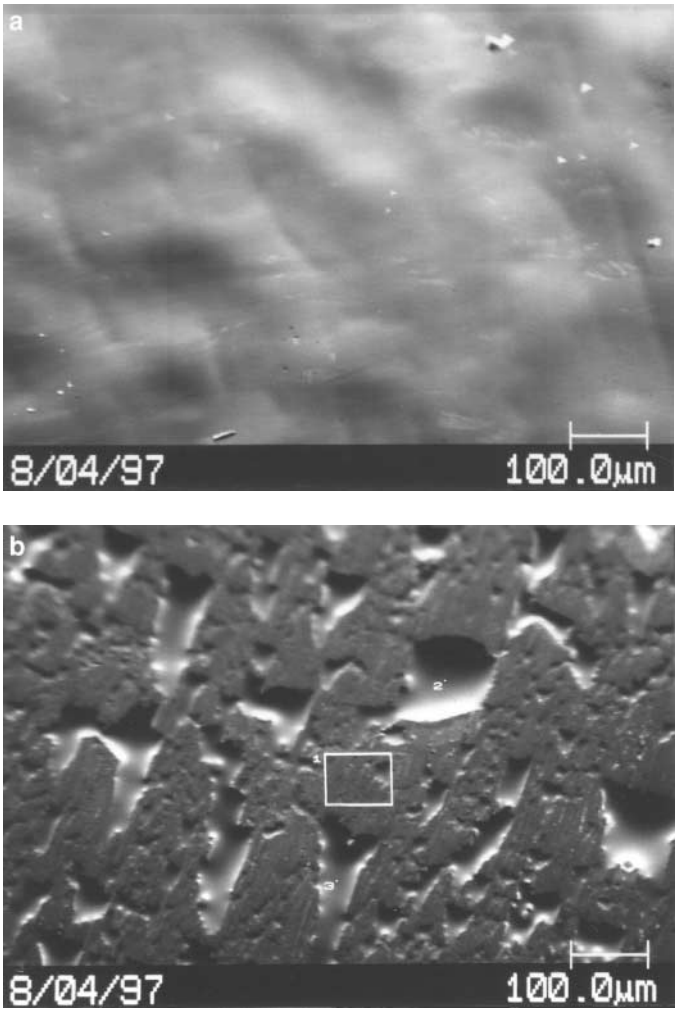

FIG. 2. Characteristic surfaces of a Ni–Al–Si–B amorphous alloy cathode prepared by rapid solidification: (a) free surface; (b) contact surface. Scanning electron micrographs.

at a scan rate of 0.02 $V\,s^{-1}$. Calibration measurements showed that the magnitude of the reduction potential was not shifted as a function of scan rate in the range 0.005–0.050 $V\,s^{-1}$. At $p_H = 1$ within the potential range investigated the proton reduction proceeds at a noticeable rate, whereas in the neutral range at $p_H \approx 6.8$ this reduction can still be neglected (Figs. 5 and 6, dashed curves). The so-called zero current in the pure electrolytes as a function the potential at every cathode was measured first for the unambiguous subsequent determination of the reduction current density $j(E)$ and, thus, of the reduction potential. In the cyclic voltammograms of 1-nitropropane, only one reduction peak was found at $p_H = 6.8$, while two reduction peaks could be discerned and measured separately at $p_H = 1$. Possibly the other reduction peaks (at potentials < -1 V vs NHE) remain invisible since they are masked by the reduction current of the protons.

The cathode consisted of a strip of the material to be tested which was covered with paraffin foil such that an

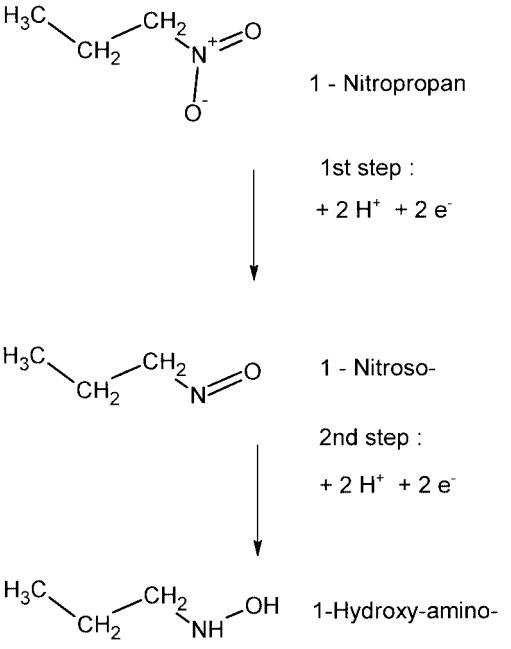

FIG. 3. Reduction sequence of 1-nitropropane.

effective surface of 28 mm^2 was exposed to the electrolyte. A Pt sheet with a surface of 600 mm^2 served as the anode. First, each cathode was cleaned in chloroform and was cycled in the pure electrolyte at least 5 times. Only the first and second cycle showed a small difference in the potential/current curves, which can be attributed to the reduction of an oxide film on the surface. After these five cycles, the reactant 1-nitropropane was added to the electrolyte and

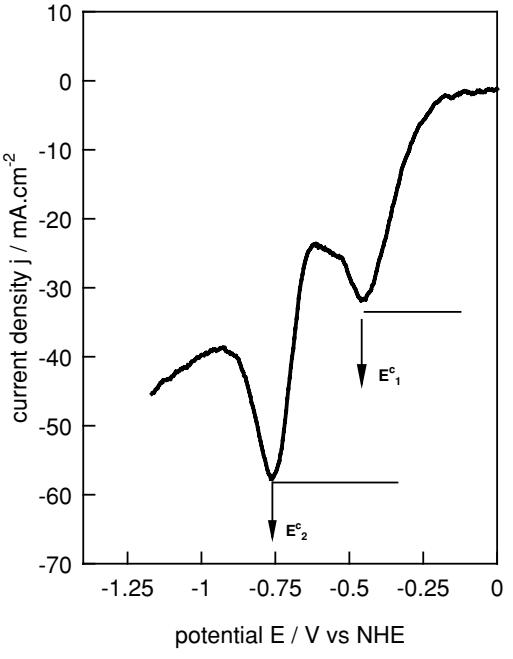

FIG. 4. Schematic plot of the electrocatalytic reduction of 1-nitropropane.

stirred until it had dissolved to saturation. The experimental scatter of the reduction potential E_n from the repetition of measurements on the same specimen was determined to be ±0.01 V.

RESULTS

Typical reduction branches of the CV curves obtained at different cathodes and at two different p_H levels are shown in Figs. 5 and 6. In Fig. 5, at $p_H = 1$, the dashed curves resulting from measurements in the pure electrolyte exhibit a "step" at about −0.3 V vs NHE which can be attributed to the incipient reduction of protons. In Fig. 6, at pH 6.8, in the range up to a potential of about −0.85 to −0.9 V vs NHE no reduction process is indicated. Obviously, in the neutral medium the reduction reaction of the H^+ ions is shifted to a more negative potential.

After addition of 1-nitropropane at $p_H = 1$, Fig. 5, two reduction peaks can be found in the potential range examined, while only one peak can be observed at $p_H = 6.8$, Fig. 6. Due to the intensive hydrogen evolution the other steps at lower potentials cannot be revealed. The reduction peaks of the 1-nitropropane are unusually wide. The mean peak width at half-height of the first reduction peak amounts to $\Delta E_{\text{eff}} = (0.160 \pm 0.016)$ V compared to a theoretical value of $\Delta E_o = 0.056$ V. Therefore, the transfer current density in the peak minimum cannot be an exact measure of the electron transfer. Nevertheless, a value of 1.72 . . . 1.87 V could be estimated based on the Randles–Sevcik equation. This indicates a two electron transition which corresponds to the reaction scheme given in Fig. 3. Peak broadening can be caused both by impeded adsorption processes and by electron transfer behavior at the electrode surface. All reduction potentials measured in the present investigation are listed in Table 2.

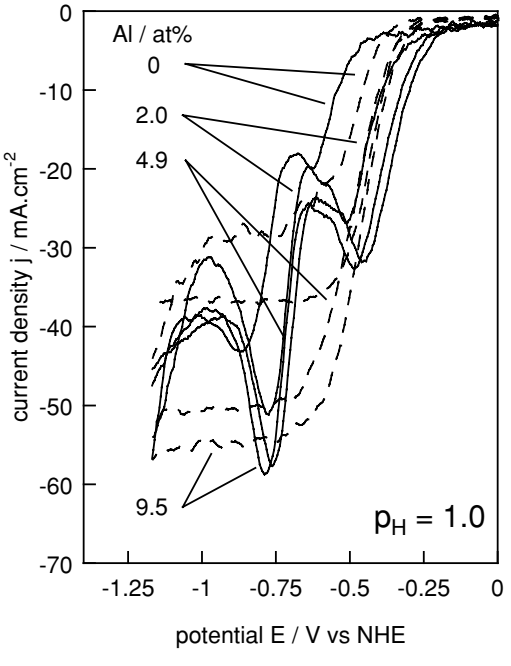

FIG. 5. Electrocatalytic reduction of 1-nitropropane at crystalline Ni–Al alloy surfaces, $p_H = 1.0$. Dashed lines, pure electrolyte; solid lines, after addition of 1-nitropropane; scatter, ±0.05 V.

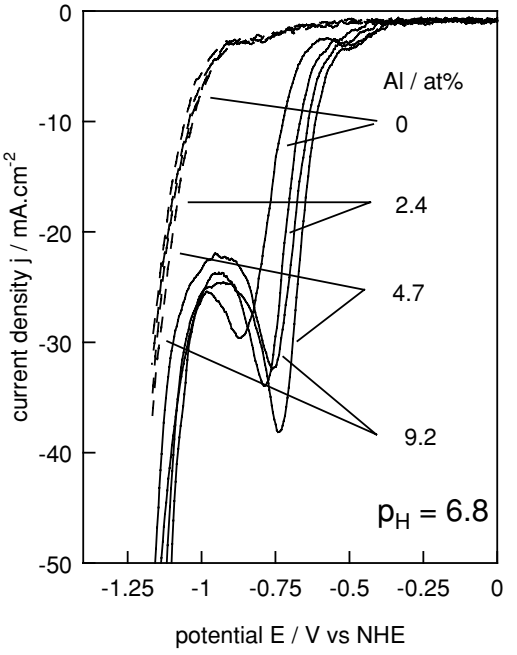

FIG. 6. Electrocatalytic reduction of 1-nitropropane at crystalline Ni–Al alloy surfaces, $p_H = 6.8$. Dashed lines, pure electrolyte; solid lines, after addition of 1-nitropropane; scatter, ±0.05 V.

TABLE 2

Results of Electrochemical Reduction Experiments

Sample designation		Reduction potential E_p^c, V vs NHE		
		$p_H = 1$		$p_H = 6.8$
No.	Designation	1st step	2nd step	1st step
K10	$Ni_{100.0}$	−0.628	−0.876	−0.870
K1	$Ni_{98.0}Al_{2.0}$	−0.512	−0.778	−0.850
K2	$Ni_{95.1}Al_{4.9}$	−0.469	−0.761	−0.860
K3	$Ni_{90.4}Al_{9.6}$	−0.471	−0.787	−0.830
E1	$Ni_{94.1}Al_{4.5}Fe_{1.4}$	−0.350	−0.780	−0.820
K6	$Ni_{91.6}Al_{4.9}Fe_{3.5}$	−0.487	−0.838	
K7	$Ni_{99.5}Pd_{0.5}$	−0.324	−0.548	−0.570
K8	$Ni_{99.0}Pd_{1.0}$			−0.590
K9	$Ni_{98.1}Pd_{1.9}$			−0.580
N10	$Ni_{74.4}Si_{7.7}B_{19.8}$	−0.374	−0.876	−0.870
N1	$Ni_{72.2}Al_{1.8}Si_{7.6}B_{17.9}$	−0.669	−0.896	−0.990
N2	$Ni_{70.7}Al_{3.5}Si_{7.8}B_{18.0}$	−0.660	−0.830	−0.950
N3	$Ni_{68.0}Al_{6.9}Si_{7.5}B_{17.6}$	−0.723	−0.924	−1.000
N6	$Ni_{68.6}Al_{3.5}Fe_{2.7}Si_{7.7}B_{19.8}$	−0.723	−0.953	−1.040
N7	$Ni_{74.6}Pd_{0.3}Si_{7.8}B_{20.0}$	−0.405	−0.644	−0.570
N9	$Ni_{72.5}Pd_{1.4}Si_{7.8}B_{20.0}$	−0.374	−0.626	−0.540
L18	$Ni_{72.6}Al_{3.8}B_{23.6}$	−0.836		−0.830
L19	$Ni_{70.0}Al_{3.7}B_{27.3}$	−0.850		−0.850
L20	$Ni_{68.8}Al_{4.0}Si_{19.5}$	−0.831		−0.880
L21	$Ni_{72.5}Al_{3.9}Si_{24.2}$	−0.757		−0.890

In Figs. 7 and 8 the data for E_p^c of Table 2 are plotted as a function of the metallic alloy concentration. The observations may be summarized as follows:

1. Pd additions to Ni raise the reduction potential E_p^c to the least negative values corresponding to the highest reactivity of all alloys investigated. There is neither a significant composition dependence between 0.5 and 2 at% Pd nor a measurable difference between the crystalline and amorphous alloys, as observed at $p_H = 6.8$, Fig. 8.

2. The most prominent feature of the Ni–Al alloy series is the different level of the reduction potential when comparing the crystalline (K series) to the amorphous (N series) alloys. The amorphous alloys exhibit a more negative reduction potential by -0.1 up to -0.2 V at both p_H levels and for both reduction steps at all Al concentrations indicating a lower activity of the amorphous alloys.

3. Regarding the effect of the Al content in solid solution in the Ni base alloys on their activity at $p_H = 1$ there is a clear initial increase with Al content ($0 < m\%$ Al < 2) for the crystalline alloys. The apparent tendency of a further increase for the crystalline and of a decrease for the amorphous alloys, at both levels of p_H, is hardly beyond the experimental scatter (± 0.05 V). Thus, these effects of composition may not be significant, at least they cannot be derived unambiguously with the method employed.

4. The addition of Fe (N6, K6) shows no clearly discernible effect on the activity beyond experimental error even though a tendency to lowering the activity of the amorphous alloys may be derived if the data points are taken at face value.

5. It is interesting to note that the activity of the single crystal specimen (E1) tends to be higher for both reduction peaks at $p_H = 1$ compared to a polycrystalline sample of similar composition. This would indicate that the {111} planes of the fcc lattice of these Ni alloys is more highly reactive than the other crystal orientations. But this would have to be substantiated by further experiments.

6. The concentration variations of the L series alloys, containing either B or Si at different levels while Al was kept constant, showed no significant effects of the kind and concentration of the metalloid elements.

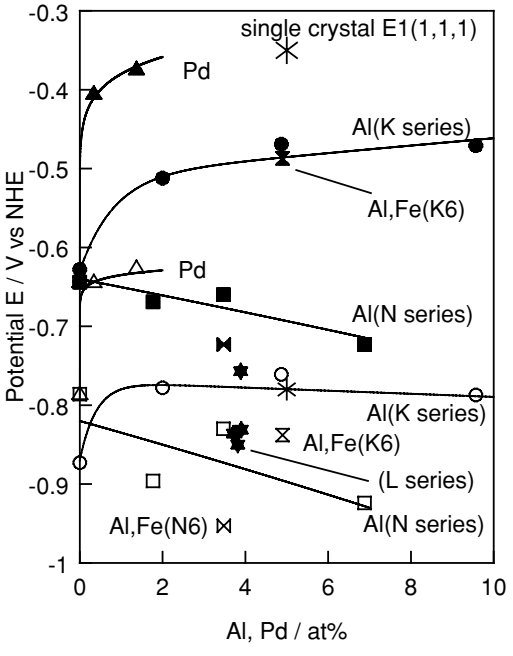

FIG. 7. Concentration dependence of the reduction potentials of 1-nitropropane at different crystalline and amorphous Ni-base alloy surfaces, $p_H = 1.0$. (full symbols) 1st step; (open symbols) 2nd step.

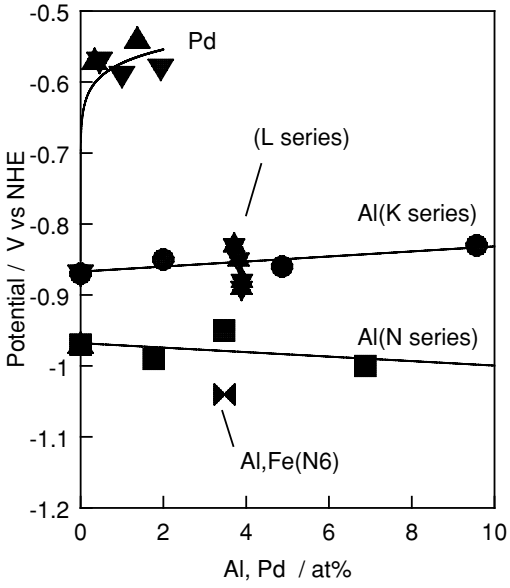

FIG. 8. Concentration dependence of the reduction potentials of 1-nitropropane at different crystalline and amorphous Ni-base alloy surfaces, $p_H = 6.8$, first reduction step.

DISCUSSION

The mechanism and the rate of heterogeneous electrochemical reduction depend on the effects of electrode properties, of electrode potential, and of the properties of the reactant on the electron transfer on the one hand, and on the concentration in the adsorption layer, its structure, and steric arrangement on the cathode surface on the other hand. Therefore the complete process is determined by the composition of the electrolyte, the type of the medium, the structure of the electrode surface, the temperature etc.

The Nernstian equation describes reversible electrochemical reactions:

$$E^{o\prime} = E^{o} - (RT/nF)^{*} \ln(A_r/A_o), \qquad [1]$$

where E^o is the standard potential of the reversible reaction, A_o and A_r are the activities of the initial and the final

product, respectively. Under identical experimental conditions the measurable effective potential $E^{o\prime}$ (rather than the thermodynamically defined quantity E^{o}) may be used for the characterization of the electron transfer at the cathode and, thus, of the electronic structure at its surface. The effective reduction potentials at different cathodes measured for a suitable test substance can be compared directly, if the reaction conditions (such as the p_H, temperature, concentration) which influence the reaction mechanism and kinetics are held sufficiently constant.

In principle, the electrochemical reduction of organic substances in aqueous systems can proceed by 2 different mechanisms (6):

1. Reduction of protons to atomic hydrogen, its absorption in the electrode metal and reaction between this stored hydrogen and the adsorbed substance S (electrocatalytic hydrogenation, ECH mechanism) :

(a) $H^+ + e^- \rightarrow H$
(b) $H + S \rightarrow$ reduced substance.

2. Direct electron transfer from the cathode to the adsorbed substance S and subsequent addition of protons (electronation–protonation, EP mechanism):

(a) $S + e^- \rightarrow S^-$
(b) $S^- + H^+ \rightarrow$ reduced substance.

Which of these two mechanisms is realized under a given set of conditions depends on the properties both of the substance to be reduced and of the cathode material (6). If the reduction potential of the protons on the cathode is more positive (including overpotential) than the reduction potential of the substance itself, the first mechanism (ECH) is realized with great probability. In this case the proneness of the cathode material to hydrogen absorption plays a certain role and the magnitude of the respective overpotentials of the proton reduction would be an indication of the catalytic activity. According to (10) the higher capacity for hydrogen absorption of a crystalline $Fe_{80}B_{20}$ alloy accounts for its higher catalytic activity. For Raney Ni and Devarda Cu catalysts Delair *et al.* (14) assume that only an ECH mechanism is operative.

From our experimental results it may be concluded that the mechanism of the reduction of nitropropane depends on the p_H of the different electrolytes used. Whereas in the case of high proton concentration the reduction of nitropropane sets on at nearly the same potential as the hydrogen formation, in neutral electrolytes a measurable difference between these potentials exists. The reduction step of the protons (reaction 1a), clearly seen at $p_H = 1$ at a potential of about -0.25 V vs NHE, disappears in the presence of 1-nitropropane, possibly because the intermediarily evolved hydrogen atoms react at a high rate with the absorbed nitropropane and 2 reduction peaks appear, Fig. 5. In the neutral medium at $p_H = 6.8$, Fig. 6, the reduction of the nitropropane takes place at a potential more positive than the potential of the proton reduction, i.e., at about -0.7 V vs NHE, compared to about -0.9 V vs NHE for the protons. Under these conditions, a direct reduction of nitropropane without the intermediate step of the formation of active hydrogen could occur (EP mechanism).

In these two cases the rate and the mechanism of the catalytic reaction as well as the measured reduction potential depend on two different sets of factors of influence: in the first case on the properties of the electrode material, its hydrogen overvoltage, the capability for the hydrogen consumption, as well as the activity of the absorbed hydrogen atoms; in the second case on the reduction potential of the test substance itself. In the case of Pd containing Ni alloys at electrodes of the K series a somewhat more positive reduction potential of the protons could be detected in electrolytes at $p_H = 1$, Fig. 7, whereas for the other alloys and at $p_H = 6.8$ no significant influence was observed. This fact may be attributed to the higher "hydrogen activity" of the Pd in the respective alloys. An ECH mechanism of reduction is realised and thus the higher electrocatalytic activity of these alloys, Figs. 7 and 8, could be explained.

CONCLUSIONS

The experimental results show that cyclic voltammetry is suitable to analyze the influence of the structure—crystalline or amorphous—and the chemical composition of the cathode material on the electrocatalytic activity of the Ni based alloys investigated. Both the amorphous and the crystalline state and the alloy composition showed a definite influence on the catalytic activity in the electrochemical reduction test reaction. The effectiveness of composition variations is weak in the case of Ni–Al alloys and strong for the Pd additions. Moreover, this influence is more marked in the case of crystalline alloys than in the case of amorphous alloys. In the acidic electrolyte ($p_H = 1$) at all electrodes, i.e., also with the Ni–Al alloy series, a tendency to more positive potentials, i.e., a decrease in the hydrogen overvoltage, compared to the pure nickel electrodes, could be observed; this influence is strong initially and hardly increases further with increasing alloy concentration.

The catalytic effect of the difference in structure is striking. Given the absence of an effect of the metalloid concentration as indicated by the results from the L series, it can be concluded that in the present alloy system the crystalline state is definitely more active catalytically than the amorphous state for the test reaction employed. Furthermore, the effect of the Al content is to increase the activity in the crystalline state and to decrease it in the amorphous state.

ACKNOWLEDGMENTS

We are grateful to U. Kühn for the preparation and metallographic characterization, and to N. Mattern for the structural characterization of the specimens.

REFERENCES

1. Kawashima, A., Hashimoto, K., and Matsumoto, T., *Corros. Houston* **39**, 577 (1980).
2. Molnár, A., Smith, G. V., and Bartók, M., *Adv. Catal.* **36**, 329 (1989).
3. Baiker, A., *Topics Appl. Phys.* **72**, 121 (1994).
4. Tsirlina, G. A., Petrii, O. A., and Kopylova, N. S., *Soviet Electrochem.* **26**(9), 949 (1990).
5. Lian, K., Kirk, D. W., and Thorpe, S. J., *Electrochim. Acta* **36**, 537 (1991).
6. Robin, D., Comtois, M., Martel, A., Lemieux, R., Amoy Kam Cheong, Belot, G., and Lessard, J., *Can. J. Chem.* **68**, 1218 (1990).
7. Vracar, L., Burojevic, S., and Krstajic, N., *J. Serb. Chem. Soc.* **63**(3), 201 (1998).
8. Kreysa, G., and Hakansson, B., *J. Electroanal. Chem.* **201**, 61 (1986).
9. Kreysa, G., Hakansson, B., and Edkunge, P., *Electrochim. Acta* **33**(10), 1351 (1988).
10. Kreysa, G., Gomez, J., Baro, A., and Arvia, A. J., *J. Electroanal. Chem.* **265**, 67 (1989).
11. Naka, M., Hashimoto, K., Masumoto, T., and Okamoto, I., rapidly quenched metals, *in* "Proc. 4th Int. Conf.," Vol. 2., p. 1431, 1981.
12. Vasiljev, V. J., and Chechetkin, A. J., *Zashch. Met.* **25**, 590 (1989).
13. Kumagai, N., Kawashima, A., and Asami, K., *J. Appl. Electrochem.* **16**, 565 (1986).
14. Delair, P., Cyr, A., and Lessard, J., "Electroorganic Synthesis: Festschrift for M. M. Baizer," p. 129. Dekker, New York, 1991.
15. Degussa A. G., test specification A301, 1991.